JACS
JOURNAL OF THE AMERICAN CHEMICAL SOCIETY

Article

pubs.acs.org/JACS

Conversion of Aldehyde to Alkane by a Peroxoiron(III) Complex: A Functional Model for the Cyanobacterial Aldehyde-Deformylating Oxygenase

Alireza Shokri and Lawrence Que, Jr.*

Department of Chemistry and Center for Metals in Biocatalysis, University of Minnesota, Minneapolis, Minnesota 55455, United States

Supporting Information

ABSTRACT: Cyanobacterial aldehyde-deformylating oxygenase (cADO) converts long-chain fatty aldehydes to alkanes via a proposed diferric-peroxo intermediate that carries out the oxidative deformylation of the substrate. Herein, we report that the synthetic iron(III)-peroxo complex $[Fe^{III}(\eta^2\text{-}O_2)(TMC)]^+$ (TMC = tetramethylcyclam) causes a similar transformation in the presence of a suitable H atom donor, thus serving as a functional model for cADO. Mechanistic studies suggest that the H atom donor can intercept the incipient alkyl radical formed in the oxidative deformylation step in competition with the oxygen rebound step typically used by most oxygenases for forming C−O bonds.

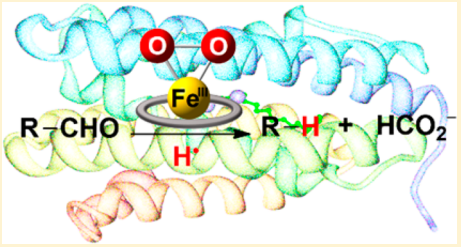

INTRODUCTION

The biosynthesis of diesel-chain alkanes and alkenes has attracted interest in recent years[1−4] because of their potential to serve as a drop-in replacement for fossil fuels.[5] Although it is quite challenging for a cell to make unfunctionalized paraffins,[6] nature synthesizes them by employing a wide variety of biochemical reactions such as dehydrations, double bond reductions, and decarboxylations. Of particular interest is the conversion of long-chain fatty aldehydes to corresponding alkanes that is catalyzed by cyanobacterial aldehyde-deformylating oxygenase (cADO).[7,8] From a structural perspective, the cADO enzyme belongs to the family of ferritin-like nonheme diiron-carboxylate enzymes that include methane monooxygenase (MMO), class I ribonucleotide reductase (RNR), and stearoyl-acyl carrier protein Δ9-desaturase (Δ9D), all of which share a common $Fe_2(His)_2(O_2CR)_4$ active site.[9,10] At first glance, it seems odd for the C−H-bond-forming cADO to be part of a family of O_2-activating enzymes that in many examples cleave C−H bonds, but it has been shown to require O_2 to carry out the oxidative deformylation of substrate to form alkane and formate (Figure 1A). In fact, isotope labeling studies[11−14] have shown that the formate product derives an O atom from O_2 and retains the aldehyde C−H bond and that the terminal methyl group of the alkane product incorporates an H atom from solvent. These observations have led to the proposed mechanism shown in Figure 1B,[15] in which O_2 binds initially to the reduced diiron center to form an adduct best described as a peroxodiiron(III) species designated as **B**. Intermediate **B** carries out a nucleophilic attack at the aldehyde carbon of the substrate to generate peroxyhemiacetal species **C**. Decay of **C** by O−O bond homolysis leads to C−C bond scission to form formate and the corresponding C_{n-1} alkyl radical, which in turn is converted to the alkane product by proton-coupled electron transfer from an iron-bound water.

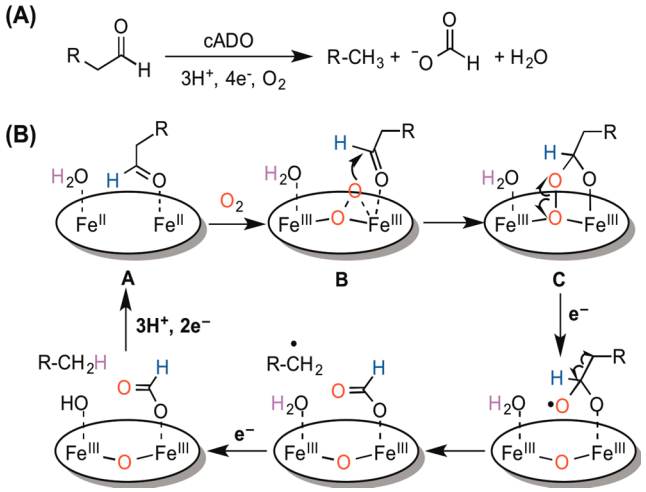

Figure 1. (A) cADO-catalyzed reaction. (B) Proposed mechanism, adapted from ref 15.

Support for the formation of a substrate-derived radical has been obtained from a substrate analog that has a cyclopropyl moiety adjacent to the putative carbon radical site and affords a ring-opened product.[16]

To date, **B** is the only intermediate in the cADO mechanism that has been trapped.[17] Its spectroscopic properties resemble those of peroxo intermediates of AurF and CmlI, diiron enzymes that catalyze the oxidation of aminoaryl substrates to nitroaryl products.[18,19] These three peroxo intermediates are distinct from corresponding intermediates of MMO, RNR, and

Received: January 30, 2015
Published: June 1, 2015

DOI: 10.1021/jacs.5b01053
J. Am. Chem. Soc. 2015, 137, 7686−7691

Δ9D, which exhibit broad visible absorption maxima near 700 nm that is associated with a (μ-1,2-peroxo)diiron(III) species.[20−22] The three more recently characterized intermediates have significantly more blue-shifted visible features near 500 nm that suggest a different peroxo binding mode.[17−19] Recently reported resonance Raman data on the CmlI-peroxo intermediate reveal a ν(O−O) at much lower energy than that found for peroxo intermediates of other nonheme diiron enzymes, for which a novel (μ−η^1:η^2-peroxo)diiron(III) unit has been proposed.[19] The mechanism proposed for cADO[15] suggests the possibility of a similar binding mode for the bound O_2 in the cADO-peroxo intermediate to endow it with sufficient nucleophilic character to attack the substrate aldehyde.

Peroxoiron(III) intermediates involved in biological transformations can have ambiphilic character.[23−27] For example, the cytochromes P450 that are involved in steroid biosynthesis generally carry out C−H bond hydroxylations via an electrophilic oxidant called compound I, derived from the activation of a peroxoiron(III) intermediate. In some reactions, however, this intermediate is proposed to be involved in the nucleophilic attack of substrate carbonyl groups resulting in C−C bond cleavage,[24,25] namely progesterone 17α-hydroxylase-17,20-lyase in the cleavage of the C17 side chain of progesterone to form androstenedione and aromatase in the conversion of testosterone to estradiol. By analogy to the latter cytochromes P450, the cADO-peroxo intermediate is proposed to carry out a nucleophilic attack on the fatty aldehyde carbonyl group to initiate its oxidative deformylation and afford the corresponding C_{n-1} alkane as the final product. This outcome is different from that observed for the heme enzymes, where the substrate has undergone partial oxidation to form a C=C or a C=O bond, rather than reduction to the alkane produced by cADO.

There is no biomimetic example to date of the reaction catalyzed by cADO. Our goal has been to test the viability of the key mechanistic step in the proposed cADO mechanism that generates alkane, where the incipient alkyl radical produced in the oxidative deformylation step is reduced to the alkane product. So far, no synthetic peroxodiiron(III) complex has been identified to have the (μ−η^1:η^2-peroxo) binding mode proposed for cADO intermediate **B** in Figure 1.[28,29] We thus initiated our cADO modeling effort with the well-characterized $[Fe^{III}(TMC)(\eta^2\text{-}O_2)]^+$ complex (**1**) (TMC = tetramethylcyclam; Figure 3),[30−32] which is one of several examples of synthetic mononuclear nonheme ferric complexes with a side-on-bound peroxo ligand.[33−42] Some $[M^{III}(\eta^2\text{-}O_2)]^+$ complexes have been shown to convert 2-phenylpropionaldehyde (PPA) to acetophenone,[31,43,44] but alkane formation has not been reported. Following precedents in heme chemistry, oxidative deformylation of an aldehyde by **1** may proceed by initial formation of a peroxohemiacetal adduct analogous to that shown for **C** in Figure 1, followed by O−O bond homolysis to generate formate, an alkyl radical, and an $Fe^{IV}(O)$ moiety; the latter two would then combine in a rebound step to form an alcohol product. With this mechanistic hypothesis in mind, we have sought to define reaction conditions under which the incipient alkyl radical may be intercepted to afford an alkane product before undergoing rebound. In this report we demonstrate that the reaction of aldehydes with **1** in THF solvent in the presence of suitable H atom donors results in the conversion of aldehydes into corresponding (n − 1) alkanes. This system thus represents the first functional model for cADO and has allowed us to gain mechanistic insights into this novel transformation.

EXPERIMENTAL SECTION

General. All reagents and solvents were purchased from Sigma-Aldrich Company and were used as received except tributyltin deuteride, which was obtained from Alfa Aesar Company. THF was degassed and stored inside of the glovebox to keep the oxygen away from it. All solution preparations were carried out under N_2 atmosphere in a glovebox. The $Fe^{II}(TMC)(OTf)_2$ complex was prepared as previously reported.[45] Reactions were carried out in septum-sealed 1 dram vials. For product analysis, the reaction mixture was passed through a short plug of silica gel prior to the GC or GC-MS analysis to remove the iron complex. Products were identified by comparing with authentic samples, and yields were determined by comparison against standard curves prepared with authentic samples and using dodecane as an internal standard.

Instrumentation. GC-MS spectra were obtained with an HP 6890 GC (HP-5 MS column, 30 m) with an Agilent 5973 mass analyzer, an Agilent Technologies 7890AGC system, and 5975C VL MSD. Ammonia was used as the ionization gas for chemical ionization analysis. A PerkinElmer AutoSystem gas chromatograph (AT-1701 column, 30 m) with a flame ionization detector was used to record gas chromatograms. UV−vis spectra were recorded on a Hewlett-Packard (Agilent) 8453 diode-array spectrophotometer (190−1100 nm range) using a Unisoku cryostat cooled by liquid nitrogen. High-resolution mass spectra were obtained via an electrospray ionization−time-of-flight mass spectrometer. ^{31}P NMR spectra were recorded on a VI-300 MHz instrument.

RESULTS AND DISCUSSION

Reactivity of PPA with $[Fe^{III}(TMC)(\eta^2\text{-}O_2)]^+$. Complex **1** was generated in situ using the reported procedure by treating 1.0 mM $Fe^{II}(TMC)(OTf)_2$ with 2.5 equiv of Et_3N followed by 5.0 equiv of H_2O_2 at −10 °C under N_2,[31] but with THF as the solvent instead of the more commonly used acetonitrile (MeCN) or trifluoroethanol (TFE) solvents. Because of the solvent change, the λ_{max} of **1** was red-shifted to 880 nm (Figure 2). This solution was quite stable at −10 °C, but the 880 nm

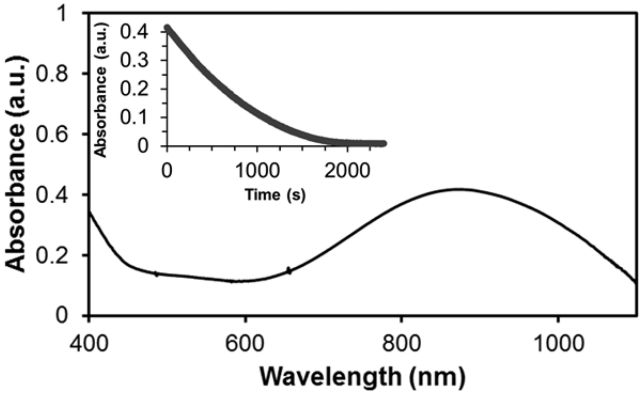

Figure 2. UV−vis spectrum of **1** obtained upon addition of 5.0 equiv of H_2O_2 to a solution containing $[Fe(TMC)]^{2+}$ (1.0 mM) and Et_3N (2.5 equiv) at −10 °C in THF. Inset: exponential decay of **1** upon addition of 100 equiv of PPA.

chromophore decayed exponentially upon treatment with PPA, resulting in the concomitant formation of 0.6 equiv of acetophenone. This amount of product was obtained with as little as 3.0 equiv of H_2O_2 and did not increase with more equiv of H_2O_2. The acetophenone likely derives from the $2e^-$ oxidation of an initially formed α-phenethanol product

DOI: 10.1021/jacs.5b01053
J. Am. Chem. Soc. 2015, 137, 7686−7691

generated from the combination of a nascent α-phenethyl radical (**Bn**•) with the $Fe^{IV}(O)$ moiety generated in the course of the reaction.

We then sought to identify conditions under which this putative radical may be intercepted and reduced to the corresponding alkane and found that ethylbenzene formed in addition to acetophenone upon addition of *n*-Bu_3SnH (125 equiv, BDE(Sn−H) = 76 ± 2 kcal mol^{-1})[46,47] to the reaction mixture (Figure S1). This product was identified by GC-MS analysis of the reaction mixture, which revealed a new peak in the GC trace that coeluted with ethylbenzene and gave rise to a protonated molecular ion at m/z = 107.2 (Figure S2A). A control experiment consisting of a mixture of *n*-Bu_3SnH and PPA did not generate any ethylbenzene. When the reaction was carried out with *n*-Bu_3SnD (96% D), deuterium was incorporated into the ethylbenzene product as indicated by GC-MS analysis (Figure S2B). The ethylbenzene yield decreased by 40%, and the mass spectral analysis showed a 1:3 ratio of the all-protio and the monodeuterio products. Analysis of these results suggests an H/D KIE of 7 for the cleavage of the Sn−H/D bond by the incipient **Bn**• radical.

Interestingly, the formation of ethylbenzene was observed only with THF as solvent, and the use of other solvents such as TFE, 1-butanol, acetone, or acetonitrile did not result in PhEt formation and formed acetophenone as sole product. Thus, only in THF was the lifetime of the incipient alkyl radical sufficiently lengthened to allow its interception by *n*-Bu_3SnH. To the best of our knowledge, this is the first report of a peroxo-iron(III) complex that can convert RCHO to R−H (Figure 3) as proposed for cADO (Figure 1).

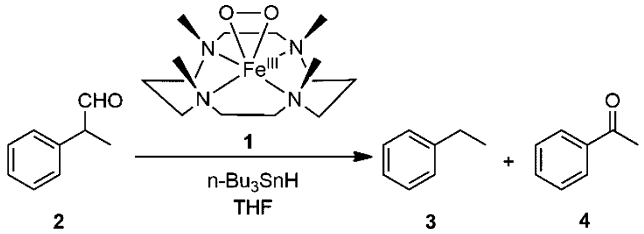

Figure 3. Reaction of $[Fe^{III}(TMC)(\eta^2\text{-}O_2)]^+$ (**1**) with PPA (**2**) in the presence of *n*-Bu_3SnH.

The effect of *n*-Bu_3SnH concentration on the reaction was explored. The [ethylbenzene]/[acetophenone] ratio increased with *n*-Bu_3SnH concentration and was maximized above 50 mM (Figure 4A), strongly suggesting that there is a competition between *n*-Bu_3SnH and the $Fe^{IV}(O)$ intermediate for trapping of the incipient **Bn**• radical, undergoing either H atom transfer from *n*-Bu_3SnH or recombination with the $Fe^{IV}(O)$ species in the "oxygen rebound" step. The saturation behavior observed as a function of *n*-Bu_3SnH concentration may be rationalized by a solvent cage effect,[48] where the amount of ethylbenzene formed reflects the fraction of nascent **Bn**• radical that can break through the cage wall and be trapped by the radical scavenger. The fraction of escaped radical depends on properties such as shape, size, and mass as well as solvent viscosity. Such radical−cage effects are well documented in organotransition metal chemistry.[49−51]

The putative **Bn**• intermediate could also be trapped by another potential H atom donor, PhNHNHPh, which has an N−H bond dissociation energy of 73.1 kcal mol^{-1}.[52] GC-MS analysis of the reaction mixtures revealed formation of

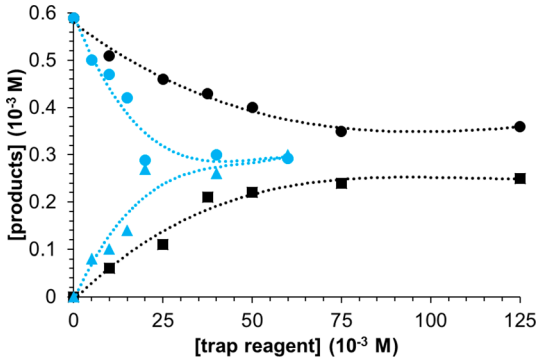

Figure 4. Product yields upon addition of *n*-Bu_3SnH (black) or Ph_3P (blue) to the reaction of **1** (1.0 mM) and PPA (20 mM) in THF at −10 °C. Circles represent the amount of acetophenone formed, squares represent the amount of ethylbenzene; and triangles represent the amount of Ph_3PO. See Table 1 for a complete list of product yields.

ethylbenzene. As found in the *n*-Bu_3SnH trapping experiments, the PhEt yield increased as the PhNHNHPh concentration increased (Table 1). A control experiment showed that this reagent also reacted quickly with **1** in the absence of the aldehyde, which may account for the lower alkane yields in these reactions relative to those obtained by *n*-Bu_3SnH interception.

Nam has demonstrated that the oxygen atom incorporated into the acetophenone product of PPA oxidation derives from the peroxo group of **1** using ^{18}O-labeling experiments.[31] To ascertain that the incipient $[Fe^{IV}(O)(TMC)]^{2+}$ species was the likely O atom source, we employed Ph_3P as a trapping nucleophile and observed the formation of Ph_3PO at the expense of acetophenone. No Ph_3PO was formed in the absence of the aldehyde. As shown in Figure 4, the $[Ph_3PO]$/[acetophenone] ratio increased with increasing $[Ph_3P]$ and leveled off above 20 mM. As with *n*-Bu_3SnH, the observed saturation is consistent with a solvent cage effect[48−51] because increasing $[Ph_3P]$ should increase the ratio until all the free (escaped) $Fe^{IV}(O)$ complex has been scavenged. Similar behavior was observed by Groves and Su for the decay of the adduct between metmyoglobin and peroxynitrite, which forms a $[Fe^{IV}(O)porphyrin/NO_2]$ pair upon rate-determining O−O bond homolysis that can undergo either NO_2 rebound to form NO_3^- or NO_2 escape and trapping by a nearby tyrosine residue.[53,54] Our results thus indicate that Ph_3P intercepts the incipient $Fe^{IV}(O)$ complex generated during the deformylation reaction.

Because the above reactions were carried out in the presence of excess of H_2O_2 and Et_3N, the reaction of PPA with isolated crystals of **1**[32] was also investigated (Table 1). Acetophenone was also formed but at half the yield, demonstrating that **1** was by itself capable of providing the four oxidizing equivalents required for the formation of ketone from PPA. ^1H NMR analysis of the solution at the end of the reaction showed no evidence for either the iron(II) or the oxoiron(IV) complex, leading us to surmise the likely formation of NMR-silent iron(III) byproducts.

All of the above experimental observations are consistent with the stoichiometry and the mechanism shown in Figure 5. Attack of **1** at the aldehyde carbonyl forms the peroxyhemiacetal intermediate. Facile homolytic cleavage of the O−O bond followed by homolytic scission of the C−C bond yields

DOI: 10.1021/jacs.5b01053
J. Am. Chem. Soc. 2015, 137, 7686−7691

Table 1. Deformylation of Aldehydes (RCHO, 20 mM) by $Fe^{III}(TMC)(\eta^2\text{-}O_2)$ (1.0 mM) in THF at −10 °C

aldehyde	conditions	[aldehyde/ketone] (mM)[a]	[alkane] (mM)[a]	[$OPPh_3$] (mM)[b]	**8** (mM)[a]
	normal	0.59			
	crystals of **1**[c]	0.33			
	n-Bu_3SnH (10 equiv)	0.51	0.06		
	n-Bu_3SnH (25 equiv)	0.46	0.11		
	n-Bu_3SnH (37.5)	0.43	0.21		
	n-Bu_3SnH (50 equiv)	0.40	0.22		
	n-Bu_3SnH (75 equiv)	0.35	0.24		
	n-Bu_3SnH (125 equiv)	0.36	0.25		
PPA	PhNHNHPh (15 equiv)	0.26	0.07		
	PhNHNHPh (100 equiv)	0.20	0.14		
	PhNHNHPh (300 equiv)	0.14	0.15		
	PPh_3 (5 equiv)	0.50		0.08	
	PPh_3 (10 equiv)	0.47		0.10	
	PPh_3 (15 equiv)	0.42		0.14	
	PPh_3 (20 equiv)	0.29		0.27	
	PPh_3 (40 equiv)	0.30		0.26	
	PPh_3 (60 equiv)	0.29		0.30	
	normal	0.09	0.26		0.28
	crystals of **1**[c]	0.05	0.06		0.06
undecanal	THF-d_8	0.13	0.15		0.16
	n-Bu_3SnH (250 equiv)	0.06	0.26		0.28
	PPh_3 (60 equiv)		0.21	0.31	0.07

[a]Determined by GC analysis. [b]Determined by ^{31}P NMR. [c]Crystals of **1** were obtained by the procedure reported in ref 45. Determination errors are approximately 10%.

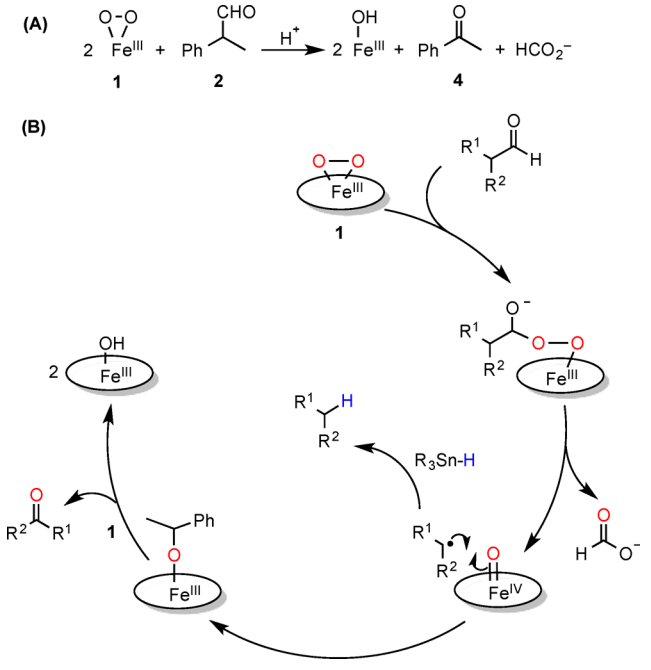

Figure 5. (A) Stoichiometry and (B) proposed mechanism for the deformylation of PPA by **1** in THF.

the $Fe^{IV}(O)$ complex, formate, and **Bn**·. The incipient radical then undergoes oxygen rebound with the newly formed $Fe^{IV}(O)$ species to form an alkoxoiron(III) complex, which is further oxidized to the ketone by a second equivalent of **1** or H_2O_2. Reaction of the alkoxoiron(III) moiety with trace water present in the solution leads to formation of $Fe^{III}(OH)(TMC)]^{2+}$, which is proposed as the byproduct of the reaction. This unstable and yet uncharacterized species very likely decays to Fe_2O_3 and free TMC, as indicated respectively by the formation of a brown precipitate in the reaction mixture and the appearance of the $[TMC\text{-}H]^+$ ion in the mass spectrum taken at the end of the reaction. The nascent alkyl radical can also react with a suitable H atom donor if present in the reaction mixture to form the observed R−H product.

Reactivity of Undecanal with $[Fe^{III}(TMC)(\eta^2\text{-}O_2)]^+$. The relatively weak C_α−H bond of PPA makes it a common substrate for the oxidative deformylation reaction. However, cADO enzyme substrates are linear aldehydes with much stronger C_α−H bonds than PPA. Consequently, undecanal was used as the model substrate in the reaction. Addition of undecanal to **1** resulted in the disappearance of its 880 nm band at a rate comparable to that for the PPA reaction. GC-MS analysis of the reaction mixture revealed three peaks, which respectively coeluted with authentic standards of decane (**6**), decanal (**7**), and γ-butyrolactone (**8**) (Figure 6 and Table 1). Although addition of excess *n*-Bu_3SnH to the reaction mixture did not affect the decane yield, substitution of THF by THF-d_8 as the reaction solvent reduced the yield of decane and resulted in deuterium incorporation into the hydrocarbon product, as determined by mass spectrometry (Figure S3). These results are consistent with the hydrogen atom coming from the solvent. Also, addition of Ph_3P to the reaction mixture prevented formation of decanal and significantly decreased the yield of the lactone derived from THF oxidation, consistent with the trapping of the $Fe^{IV}(O)$ intermediate that serves as the O atom source for these products. We were not able to establish the fate of either the decyl or the THF-derived radical in this experiment.

Formation of **6** and **7** in the undecanal experiments implies a reaction mechanism analogous to that proposed for PPA (Figure 5). However, the decyl radical ($CH_3(CH_2)_8CH_2$·) is much more reactive than **Bn**· and powerful enough to abstract an H atom from THF to generate decane. The newly formed THF radical then combines with the $Fe^{IV}(O)$ complex to form

DOI: 10.1021/jacs.5b01053
J. Am. Chem. Soc. 2015, 137, 7686−7691

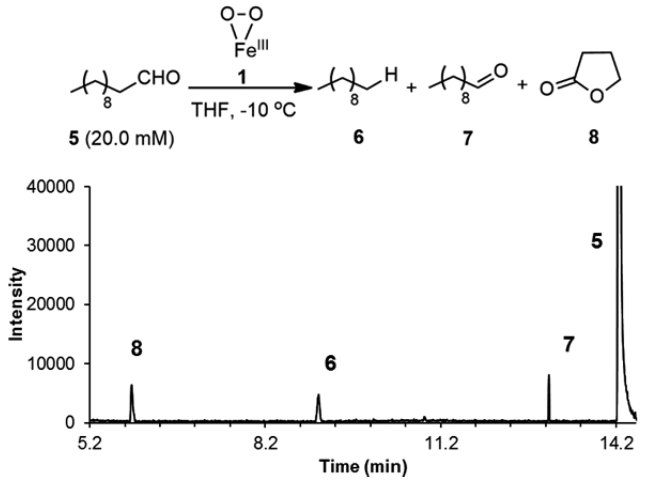

Figure 6. GC-MS traces of the products from the reaction of **1** with undecanal.

γ-butyrolactol, which in turn is oxidized to **8**. The ability of the decyl radical to abstract H• from THF is related to its thermodynamic affinity for H•, reflecting the relative strengths of the C−H bonds involved. The C_α−H bonds of THF and the primary C−H bonds of decane have respective bond dissociation energies of 92 and 98 kcal mol^{-1},[55] so H atom transfer from THF to decyl radical is favored.

Kinetic studies of the reactions of **1** with PPA or undecanal in THF at −10 °C reveal that the rate of **1** decay is independent of the nature of the aldehyde and of the concentration of the aldehyde. As shown in Figures S4 and S5, the observed k_{obs} values fall within the range of 6−10 × 10^{-4} s^{-1} under all conditions studied, with similar rates obtained using the peroxo crystals as the starting point. This behavior differs from that found by Nam for the reactions of **1** with PPA in TFE solvent, the rates of which depend on the PPA concentration.[31] We speculate that the reactivity differences of **1** in the two solvents derive from the accessibility of its more nucleophilic end-on-bound isomer. In the less polar THF solvent, formation of the end-on-bound isomer is not so favored, so the isomerization of **1** is rate-determining. However, in the more polar and hydrogen-bonding TFE solvent, isomerization is more facile, and the rate-determining step becomes the attack of **1** on the carbonyl group of the aldehyde. The importance of an end-on peroxo moiety for oxidative deformylation is emphasized by the much higher reactivity of $[Fe^{III}(TMC)(\eta^1\text{-}OOH)]^{2+}$ relative to that of **1** at −40 °C as demonstrated by Nam[32] and the very rapid oxidation of PPA by $[Fe^{III}(TMCS)(\eta^1\text{-}OO)]^{+}$ even at −90 °C, where TMCS is a pentadentate analog of TMC with a pendant thiolate donor.[44] A similar argument has been used to rationalize the significantly enhanced reactivity of $[Fe^{III}(F_{20}TPP)(\eta^2\text{-}O_2)]^{+}$ ($H_2F_{20}TPP$ = tetrakis(pentafluoro-phenyl)porphin) upon addition of DMSO, which is proposed to bind to the site trans to the peroxo ligand and promote the isomerization of the side-on bound peroxo moiety to its end-on-bound form.[56]

We have demonstrated deformylation of aldehydes by $[Fe^{III}(TMC)(\eta^2\text{-}O_2)]^{+}$ in the presence of the H atom donors to form alkanes in THF solvent, affording the first functional model for cADO. Following the previously proposed mechanism for oxidative deformylation of aldehydes,[31] we suggest that **1** reacts with RCHO by first converting to its η^1-OO^- isomer and then generating a peroxyhemiacetal adduct; this species then undergoes O−O bond homolysis to afford R•, formate, and $[Fe^{IV}(O)(TMC)]^{2+}$. At this stage, the presence of a suitable H atom donor intercepts R• to make R−H, instead of forming a C−O bond with the $Fe^{IV}(O)$ complex. The success of our cADO modeling efforts has hinged on a shift in solvent from TFE,[31] used in previous studies of aldehyde deformylation by **1**, to THF. We speculate that the change in solvent may tune the rate at which the incipient alkyl radical undergoes rebound with $[Fe^{IV}(O)(TMC)]^{2+}$ to allow the incipient alkyl radicals to be intercepted by an H atom donor. These results support the basic premise of the mechanism proposed for the cADO-catalyzed reaction,[11−13] i.e., that the aldehyde substrate is attacked by a nucleophilic iron-peroxo species formed in the cADO active site such as the $(\mu\text{−}\eta^1\text{:}\eta^2\text{-peroxo})$diiron(III) moiety **C** proposed for cADO in Figure 1. Subsequent injection of an electron concomitant with O−O bond cleavage in the decay of **C** avoids formation of an oxoiron(IV) center with which the incipient alkyl radical can undergo rebound. Instead, the radical abstracts an H atom from an iron-bound water to form the desired alkane product.

■ ASSOCIATED CONTENT

Supporting Information

Figures as described in the text. The Supporting Information is available free of charge on the ACS Publications website at DOI: 10.1021/jacs.5b01053.

■ AUTHOR INFORMATION

Corresponding Author

*larryque@umn.edu

Notes

The authors declare no competing financial interest.

■ ACKNOWLEDGMENTS

Generous support from the National Institutes of Health (GM-38767) is gratefully acknowledged.

■ REFERENCES

(1) Lam, M. K.; Lee, K. T. *Biotechnol. Adv.* **2012**, *30*, 673−690.
(2) Malcata, F. X. *Trends Biotechnol.* **2011**, *29*, 542−549.
(3) Jones, C. S.; Mayfield, S. P. *Curr. Opin. Biotechnol.* **2012**, *23*, 346−351.
(4) Kung, Y.; Runguphan, W.; Keasling, J. D. *ACS Synth. Biol.* **2012**, *1*, 498−513.
(5) Ghim, C.-M.; Kim, T.; Mitchell, R.; Lee, S. *Biotechnol. Bioprocess Eng.* **2010**, *15*, 11−21.
(6) Buist, P. H. *Nat. Prod. Rep.* **2007**, *24*, 1110−1127.
(7) Cheesbrough, T. M.; Kolattukudy, P. E. *Proc. Natl. Acad. Sci. U.S.A.* **1984**, *81*, 6613−6617.
(8) Schirmer, A.; Rude, M. A.; Li, X.; Popova, E.; del Cardayre, S. B. *Science* **2010**, *329*, 559−562.
(9) Krebs, C.; Bollinger, J. M., Jr.; Booker, S. J. *Curr. Opin. Chem. Biol.* **2011**, *15*, 291−303.
(10) Wallar, B. J.; Lipscomb, J. D. *Chem. Rev.* **1996**, *96*, 2625−2658.
(11) Das, D.; Eser, B. E.; Han, J.; Sciore, A.; Marsh, E. N. G. *Angew. Chem., Int. Ed.* **2011**, *50*, 7148−7152.
(12) Waugh, M. W.; Marsh, E. N. G. *Biochemistry* **2014**, *53*, 5537−5543.
(13) Warui, D. M.; Li, N.; Nørgaard, H.; Krebs, C.; Bollinger, J. M., Jr.; Booker, S. J. *J. Am. Chem. Soc.* **2011**, *133*, 3316−3319.
(14) Li, N.; Chang, W.; Warui, D. M.; Booker, S. J.; Krebs, C.; Bollinger, J. M., Jr. *Biochemistry* **2012**, *51*, 7908−7916.
(15) Li, N.; Nørgaard, H.; Warui, D. M.; Booker, S. J.; Krebs, C.; Bollinger, J. M., Jr. *J. Am. Chem. Soc.* **2011**, *133*, 6158−6161.

DOI: 10.1021/jacs.5b01053
J. Am. Chem. Soc. 2015, 137, 7686−7691

(16) Paul, B.; Das, D.; Ellington, B.; Marsh, E. N. G. *J. Am. Chem. Soc.* **2013**, *135*, 5234−5237.
(17) Pandelia, M. E.; Li, N.; Nørgaard, H.; Warui, D. M.; Rajakovich, L. J.; Chang, W.; Booker, S. J.; Krebs, C.; Bollinger, J. M., Jr. *J. Am. Chem. Soc.* **2013**, *135*, 15801−15812.
(18) Korboukh, V. K.; Li, N.; Barr, E. W.; Bollinger, J. M., Jr.; Krebs, C. *J. Am. Chem. Soc.* **2009**, *131*, 13608−13609.
(19) Makris, T. M.; Vu, V. V.; Meier, K. K.; Komor, A. J.; Rivard, B. S.; Münck, E.; Que, L., Jr.; Lipscomb, J. D. *J. Am. Chem. Soc.* **2015**, *137*, 1608−1617.
(20) Liu, K. E.; Valentine, A. M.; Wang, D.; Huynh, B. H.; Edmondson, D. E.; Salifoglou, A.; Lippard, S. J. *J. Am. Chem. Soc.* **1995**, *117*, 10174−10185.
(21) Broadwater, J. A.; Ai, J.; Loehr, T. M.; Sanders-Loehr; Fox, B. G. *Biochemistry* **1998**, *37*, 14664−14671.
(22) Skulan, A. J.; Brunold, T. C.; Baldwin, J.; Saleh, L.; Bollinger, J. M., Jr.; Solomon, E. I. *J. Am. Chem. Soc.* **2004**, *126*, 8842−8855.
(23) White, R. E.; Coon, M. J. *Annu. Rev. Biochem.* **1980**, *49*, 315−356.
(24) Groves, J. T. *Ann. N.Y. Acad. Sci.* **1986**, *471*, 99−107.
(25) Guengerich, F. P.; Macdonald, T. L. *Adv. Electron Transfer Chem.* **1993**, *3*, 191−241.
(26) Wertz, D. L.; Valentine, J. S. *Struct. Bonding (Berlin, Ger.)* **2000**, *97*, 37−60.
(27) Sono, M.; Roach, M. P.; Coulter, E. D.; Dawson, J. H. *Chem. Rev.* **1996**, *96*, 2841−2887.
(28) Cranswick, M. A.; Meier, K. K.; Shan, X.; Stubna, A.; Kaizer, J.; Mehn, M. P.; Münck, E.; Que, L. *Inorg. Chem.* **2012**, *51*, 10417−10426.
(29) Fiedler, A. T.; Shan, X.; Mehn, M. P.; Kaizer, J.; Torelli, S.; Frisch, J. R.; Kodera, M.; Que, L., Jr. *J. Phys. Chem. A* **2008**, *112*, 13037−13044.
(30) Cho, J.; Sarangi, R.; Nam, W. *Acc. Chem. Res.* **2012**, *45*, 1321−1330.
(31) Annaraj, J.; Suh, Y.; Seo, M. S.; Kim, S. O.; Nam, W. *Chem. Commun.* **2005**, 4529−4531.
(32) Cho, J.; Jeon, S.; Wilson, S. A.; Liu, L. V.; Kang, E. A.; Braymer, J. J.; Lim, M. H.; Hedman, B.; Hodgson, K. O.; Valentine, J. S.; Solomon, E. I.; Nam, W. *Nature* **2011**, *478*, 502−505.
(33) Girerd, J.-J.; Banse, F.; Simaan, A. J. *Struct. Bonding (Berlin, Ger.)* **2000**, *97*, 145−177.
(34) Costas, M.; Mehn, M. P.; Jensen, M. P.; Que, L., Jr. *Chem. Rev.* **2004**, *104*, 939−986.
(35) Jensen, K. B.; McKenzie, C. J.; Nielsen, L. P.; Pedersenand, J. Z.; Svendsen, H. M. *Chem. Commun.* **1999**, 1313−1314.
(36) Ho, R. Y. N.; Roelfes, G.; Hermant, R.; Hage, R.; Feringa, B. L.; Que, L., Jr. *Chem. Commun.* **1999**, 2161−2162.
(37) Simaan, A. J.; Döpner, S.; Banse, F.; Bourcier, S.; Bouchoux, G.; Boussac, A.; Hildebrandtand, P.; Girerd, J. J. *Eur. J. Inorg. Chem.* **2000**, 1627−1633.
(38) Simaan, A. J.; Banse, F.; Girerd, J. J.; Wieghardt, K.; Bill, E. *Inorg. Chem.* **2001**, *40*, 6538−6540.
(39) Hazell, A.; McKenzie, C. J.; Nielsen, L. P.; Schindler, S.; Weitzer, M. *J. Chem. Soc., Dalton Trans.* **2002**, 310−317.
(40) Horner, O.; Jeandey, C.; Oddou, J.-L.; Bonville, P.; McKenzie, C. J.; Latour, J. M. *Eur. J. Inorg. Chem.* **2002**, 3278−3283.
(41) Roelfes, G.; Vrajmasu, V.; Chen, K.; Ho, R. Y. N.; Rohde, J. U.; Zondervan, C.; la Crois, R. M.; Schudde, E. P.; Lutz, M.; Spek, A. L.; Hage, R.; Feringa, B. L.; Münck, E.; Que, L., Jr. *Inorg. Chem.* **2003**, *42*, 2639−2653.
(42) Bukowski, M. R.; Comba, P.; Limberg, C.; Merz, M.; Que, L., Jr.; Wistuba, T. *Angew. Chem., Int. Ed.* **2004**, *43*, 1283−1287.
(43) Jo, Y.; Annaraj, J.; Seo, M. S.; Lee, Y.-M.; Kim, S. Y.; Cho, J.; Nam, W. *J. Inorg. Biochem.* **2008**, *102*, 2155−2159.
(44) McDonald, A. R.; Van Heuvelen, K. M.; Guo, Y.; Li, F.; Bominaar, E. L.; Münck, E.; Que, L., Jr. *Angew. Chem., Int. Ed.* **2012**, *51*, 9132−9136.
(45) Rohde, J.-U.; In, J.-H.; Lim, M. H.; Brennessel, W. W.; Bukowski, M. R.; Stubna, A.; Münck, E.; Nam, W.; Que, L. *Science* **2003**, *299*, 1037−1039.
(46) Burkey, T. J.; Majewski, M.; Griller, D. *J. Am. Chem. Soc.* **1986**, *108*, 2218−2221.
(47) Laarhoven, L. J. J.; Mulder, P.; Wayner, D. D. M. *Acc. Chem. Res.* **1999**, *32*, 342−349.
(48) Lorand, J. P. *Prog. Inorg. Chem.* **1972**, *17*, 207−325.
(49) Braden, D. A.; Parrack, E. E.; Tyler, D. R. *Coord. Chem. Rev.* **2001**, *211*, 279−294.
(50) Koenig, T. W.; Hay, B. P.; Finke, R. G. *Polyhedron* **1988**, *7*, 1499−1516.
(51) Jacobsen, E. N.; Bergman, R. G. *J. Am. Chem. Soc.* **1985**, *107*, 2023−2032.
(52) Ingemann, S.; Fokkens, R. H.; Nibbering, N. M. M. *J. Org. Chem.* **1991**, *56*, 607−612.
(53) Su, J.; Groves, J. T. *J. Am. Chem. Soc.* **2009**, *131*, 12979−12988.
(54) Su, J.; Groves, J. T. *Inorg. Chem.* **2010**, *49*, 6317−6329.
(55) Pedley, J. B.; Naylor, R. D.; Kirby, S. P. *Thermochemical Data of Organic Compounds*, 2nd ed.; Chapman and Hall: New York, 1986.
(56) Selke, M.; Valentine, J. S. *J. Am. Chem. Soc.* **1998**, *120*, 2652−2653.

DOI: 10.1021/jacs.5b01053
J. Am. Chem. Soc. 2015, 137, 7686−7691